Non-reciprocal wave retarder based on optical rotators combination

Mouhamad Al-Mahmoud, Hristina Hristova, Virginie Coda, Andon A Rangelov, Nikolay V Vitanov, Germano Montemezzani

Research Article Vol. 4, No. 10 / 15 Oct 2021 / OSA Continuum 2695
OSA CONTINUUM

Non-reciprocal wave retarder based on optical rotators combination

MOUHAMAD AL-MAHMOUD,[1,*] HRISTINA HRISTOVA,[2] VIRGINIE CODA,[3] ANDON A. RANGELOV,[1] NIKOLAY V. VITANOV,[1] AND GERMANO MONTEMEZZANI[3]

[1]*Department of Physics, Sofia University, James Bourchier 5 blvd, 1164 Sofia, Bulgaria*
[2]*Institute of Solid State Physics, Bulgarian Academy of Sciences, 72 Tsarigradsko chaussée, 1784 Sofia, Bulgaria*
[3]*Université de Lorraine, CentraleSupélec, LMOPS, F- 57000 Metz, France*
[*]*mouhamadmahmoud1@gmail.com*

Abstract: We propose and demonstrate a method to realize an easily tunable non-reciprocal wave retarder whose phase retardation depends on the light propagation direction. The system is based on a combination of a reciprocal polarization rotator, a non-reciprocal magneto-optical rotator, and two quarter-wave plates. Experimental tests demonstrate various non-reciprocal functionalities in complete agreement with the underlying theoretical concept.

1. Introduction

A conventional wave retarder is generally composed of a transparent birefringent crystal plate inducing a phase shift between the two eigenpolarizations of the plate [1–3]. They can for instance be used to transform the state of light polarization between linear, circular or elliptical states, as often required in optical experiments and technologies. Being lossless linear optical elements, such retarders are reciprocal owing to the time reversal symmetry connected to the time reversal invariance of the underlying Maxwell equations and of the linear wave equation. Here the reciprocity has the consequence that forward and backward propagating light through the plate are subjected to the same phase shift. However there exist various optical systems capable of breaking reciprocity [4,5]. One example is found for light propagating in nonlinear optical media, for which the above time reversal symmetry no longer holds and the reciprocity breaking leads to various interesting functionalities [6–10]. Reciprocity can be broken also in some dynamic devices by taking advantage of a time-dependent refractive index capable of coupling forward propagating modes but not backward propagating ones, or vice versa [11–13].

Nevertheless, the most ubiquitous non-reciprocal elements are based on magneto-optical effects such as the Faraday effect. Here the non-reciprocity is associated to the axial (rather than polar) nature of the magnetic field and magnetization vectors and the related invariance upon space inversion. Magneto-optical effects are widely used to build optical isolators or circulators [14], both in bulk and integrated optics. Specifically, several guided wave configurations allow to achieve a non-reciprocal phase shift for the two propagation directions [15–20]. While such devices often address only one of the two polarizations (TM or TE), the use of waveguides supporting both polarization modes can lead in principle to the equivalent of a non-reciprocal wave retarder. In this case a different magneto-optically induced phase shift for the TM and TE waves can be related to the local magnetic field geometry and the different spatial distribution of the two optical waves. In contrast, Faraday rotators, the standard non-reciprocal elements used in bulk optics, rely on a magneto-optically induced circular birefringence associated to a longitudinal magnetic field. These elements belong to the category of optical rotators for which any linear state of polarization is rotated by a fixed angle which is independent of the input

#439325 https://doi.org/10.1364/OSAC.439325
Journal © 2021 Received 2 Aug 2021; revised 5 Oct 2021; accepted 5 Oct 2021; published 17 Oct 2021

OSA CONTINUUM

polarization direction. As such they differ intrinsically from wave retarder elements in terms of their functionality.

In this paper, we propose an approach to realize adjustable non-reciprocal wave retarders on the base of a non-reciprocal Faraday rotator combined to a reciprocal rotator composed of two half-wave plates. It is shown that if these elements are sandwiched between crossed quarter-wave plates they act as wave retarders with a retardation differing in forward and backward direction. The forward and backward phase shifts depend on the combined rotation angle of the rotators and can be adjusted by turning one of the half-wave plates in the reciprocal rotator. Section 2 presents the concept and its theoretical background, while Sect. 3 gives two simple examples of experimental verification using off-the-shelf optical elements.

2. Concept background

The principle of the non-reciprocal wave retarder is illustrated in Fig. 1(a) for the forward and backward light propagation directions. It consists of several elements. The two central ones are a reciprocal rotator (RR) turning a linear polarization by an angle θ_1 in forward direction (and turning it back by $-\theta_1$ in the backward direction) and a non-reciprocal Faraday rotator (FR) that turns the polarization by an angle θ_2 for both propagation directions. These two elements are sandwiched between two quarter-wave plates (QWP1 and QWP2) with their fast axes aligned along the vertical and horizontal laboratory axes, respectively.

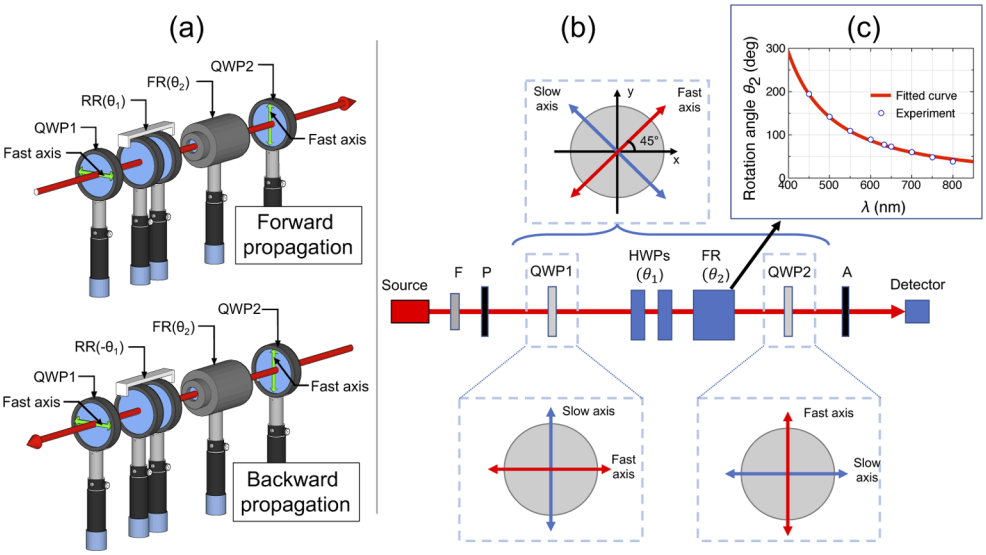

Fig. 1. (a) Non-reciprocal wave retarder sequence for forward (top) and backward (bottom) propagation direction. QWP1 and QWP2 are two crossed quarter-wave plates. RR is a reciprocal polarization rotator (rotation angle θ_1) composed of two half-wave plates (HWPs) and FR is a non-reciprocal Faraday rotator (rotation angle θ_2). (b) Scheme of the set-up for experimental verification. F: spectral filter, P: polarizer, A: analyzer. The bottom diagrams show the orientation of the fast and slow axes of the two QWPs. The top diagram shows the 45 deg orientation of the resulting effective retarder having a phase retardation $\varphi_f = 2(\theta_1 + \theta_2)$ and $\varphi_b = 2(\theta_2 - \theta_1)$ in forward and backward directions, respectively. Panel (c) gives the measured dispersion (blue circles) of the rotation angle θ_2 of the FR, as well as the fit with Eq. (8) (red curve).

In order to understand how this combination acts as a non-reciprocal wave retarder we rely on Jones calculus [2,3]. We first recall that the Jones matrix of a waveplate retarder whose axes are

OSA CONTINUUM

aligned with the laboratory axes x and y has the diagonal form

$$J(\varphi) = \begin{bmatrix} e^{i\varphi/2} & 0 \\ 0 & e^{-i\varphi/2} \end{bmatrix}, \tag{1}$$

where $\varphi = 2\pi L(n_s - n_f)/\lambda$ is the retarder phase shift between the fast and the slow polarization components, λ is the wavelength in vacuum, n_f and n_s are the refractive indices along the fast and slow axes respectively, and L is the thickness of the waveplate. If the axes of the waveplate retarder are rotated by an angle θ with respect to the laboratory axes, then its Jones matrix $J_\theta(\varphi)$ is obtained from the above Jones matrix $J(\varphi)$ by the matrix multiplication $J_\theta(\varphi) = R(-\theta)J(\varphi)R(\theta)$, so that

$$J_\theta(\varphi) = \begin{bmatrix} e^{i\varphi/2}\cos^2(\theta) + e^{-i\varphi/2}\sin^2(\theta) & -i\sin(2\theta)\sin(\varphi/2) \\ -i\sin(2\theta)\sin(\varphi/2) & e^{-i\varphi/2}\cos^2(\theta) + e^{i\varphi/2}\sin^2(\theta) \end{bmatrix}, \tag{2}$$

with the rotation matrix $R(\theta)$ in the horizontal-vertical (HV) basis given by

$$R(\theta) = \begin{bmatrix} \cos\theta & -\sin\theta \\ \sin\theta & \cos\theta \end{bmatrix}. \tag{3}$$

It is well known that a reciprocal polarization rotator can be built by combining two half-wave plates (HWP) for which $\varphi = \pi$ and oriented under the angles θ_A and θ_B [21,22]. The corresponding Jones matrix of the RR is obtained directly from (2) as

$$J_R(\theta_1) = J_{\theta_B}(\pi)J_{\theta_A}(-\pi) = \begin{bmatrix} \cos[2(\theta_B - \theta_A)] & \sin[2(\theta_B - \theta_A)] \\ -\sin[2(\theta_B - \theta_A)] & \cos[2(\theta_B - \theta_A)] \end{bmatrix} \equiv \begin{bmatrix} \cos\theta_1 & \sin\theta_1 \\ -\sin\theta_1 & \cos\theta_1 \end{bmatrix}, \tag{4}$$

where the subscript R indicates that we are dealing with a rotator matrix and θ_1 is the polarization rotation angle. Up to a minus sign in the angle $J_R(\theta_1)$ has the same form as the rotation matrix (3). As expected, the rotation angle of such a RR is $\theta_1 = 2(\theta_B - \theta_A)$ and corresponds to twice the difference between the orientation angles of the two HWPs composing it.

While such a rotator is reciprocal (propagation in the opposite direction does undo the polarization rotation), this is no longer the case if the RR is combined with a magneto-optical FR. The combination of the above RR with a FR that rotates further the polarization by an angle θ_2 will lead to a total rotation $\theta_f = \theta_1 + \theta_2$ in forward direction, and to a rotation $\theta_b = \theta_2 - \theta_1$ in backward direction, characterized by the Jones matrices $J_R(\theta_1 + \theta_2)$ and $J_R(\theta_2 - \theta_1)$, respectively. As discussed recently by Messaadi et al. [23], a tunable polarization rotator can be transformed into a tunable retarder by placing it between crossed QWPs (characterized by the Jones matrix $J_\theta(\pi/2)$). Indeed, the overall Jones matrix J_{seq} for the sequence shown in Fig. 1(a) is found as

$$J_{\text{seq}} = J_{\pi/2}(\pi/2)J_R(\theta_f)J_0(\pi/2) = \begin{bmatrix} \cos\theta_f & -i\sin\theta_f \\ -i\sin\theta_f & \cos\theta_f \end{bmatrix} = J_{\pi/4}(2\theta_f), \tag{5}$$

where the last equality can be easily verified by comparing with Eq. (2). An equivalent expression (containing the angle θ_b instead of θ_f) holds for the backward direction. It is worth noting that the above transformation is equivalent to the one connecting the rotation gate and the phase gate via the Hadamard gate in quantum information [24].

Equation (5) shows that the whole sequence acts as an effective waveplate with a phase retardation equal to

$$\varphi_f = 2\theta_f = 2(\theta_1 + \theta_2). \tag{6}$$

This effective waveplate is oriented at an angle of $\theta = 45$ deg with respect to the horizontal and vertical laboratory axes and thus also at 45 deg with respect to the orientations of the crossed

OSA CONTINUUM

input and output QWPs. The same is true for the backward direction but here the effective waveplate has a different phase retardation of

$$\varphi_b = 2\theta_b = 2(\theta_2 - \theta_1). \tag{7}$$

Therefore the arrangement acts as a non-reciprocal waveplate with retardations tunable by the orientations of the internal HWPs. The orientation of the effective non-reciprocal waveplate can be changed by rotating both external QWPs by the same amount in a common direction.

3. Experiments

Equations (6) and (7) show that in principle it is possible to realize any combination of the retardations φ_f and φ_b provided that the rotation angles θ_1 for the RR and θ_2 for the non-reciprocal FR can be adjusted independently. In this section we verify experimentally two specific cases. In the first the system acts approximately as a HWP in forward direction and as a QWP in backward direction. In the second case we consider a general wave retardation in forward direction associated to a neutral null retarder in backward direction. In our experiments the polarization rotation angle θ_2 of the FR will be varied by a change of wavelength exploiting the strong dispersion of the Verdet constant associated to the Faraday effect.

The experimental arrangement is shown schematically in Fig. 1(b). The light source is either a broadband white light source (ThorLabs SLS201L) filtered by a spectral filter (F) transmitting a bandwidth $\Delta\lambda$ = 10nm (at FWHM) or a He-Ne laser at the wavelength λ = 632.8 nm without spectral filter. The two HWPs used to realize the RR are built by the combination of two pre-calibrated adjustable liquid crystals waveplates (LCWP, ThorLabs: LCC1421-A) with the applied voltage tuned to a retardation of π for the wavelength of interest. For wavelengths different from 632.8 nm the two QWPs are composed by another LCWP and an optical compensator (ThorLabs SBC-VIS), both tuned to a retardation of $\pi/2$, while for λ = 632.8 nm two commercial QWPs at this wavelength are used. The used Faraday rotator FR (ThorLabs: IO-3-780-HP) has a central wavelength of 780 nm. We have characterized the dispersion of its rotation angle θ_2 at nine wavelengths between 450 and 800 nm using different spectral filters for the broadband source, as shown in Fig. 1(c). Here the experimentally measured rotation angles are fitted by the simplified relation usually applied to the Verdet constant [25,26]

$$\theta_2 = \frac{A}{\lambda^2 - \lambda_0^2}\,, \tag{8}$$

with A = 24.7 deg $(\mu\text{m})^2$ and an effective oscillator wavelength λ_0 = 273.8 nm. The arrangement in Fig. 1(b) corresponds to the forward direction. The backward direction is obtained by interchanging the role of the source and the detector, as well as of the input polarizer (P) and the output analyzer (A).

For the first demonstration we choose an input light filtered at the wavelength of 650 nm, for which the measured Faraday rotation of θ_2 = 72 deg is close to the ideal value of 67.5 deg that would be necessary (combined with θ_1 = 22.5 deg) for achieving at the same time an exact HWP in forward direction and an exact QWP in the backward one. In our specific case we use horizontally polarized input light, thus at an angle of 45 deg to the main axes of the resulting effective wave retarder. The rotation angle of the RR was set to θ_1 = 26 deg, this combination leads to a phase shift $\varphi_f = 1.09 \times \pi$ in forward direction and $\varphi_b = 1.03 \times \pi/2$ in backward direction, which are close to the values for a HWP and QWP, respectively. In order to characterize the function of the sequence we have measured the light extinction characteristics through an analyzer (element A in Fig. 1(b), Glan-Thompson polarizer) placed at its output. The normalized transmission through this element for the forward direction is shown in Fig. 2(a) together with the predicted theoretical transmission. The latter is obtained by projecting into the

OSA CONTINUUM

analyzer the expected output polarization (obtained by applying the Jones matrix J_{seq} in (5) to the input polarization) and taking the square modulus of the result. If the effective retarder would act exactly as a HWP the sequence would rotate the input polarization by 90 deg and lead to a vertically linearly polarized output with perfect extinction when the analyzer is in the horizontal position (angle $\beta = 0$ deg). Here the extinction is not fully complete owing to the 9% excess in phase shift as compared to a HWP resulting from the choice of the angles θ_1 and θ_2. This leads to a slight elliptical component of the output polarization. The normalized transmission for the reversed (backward) direction is shown in Fig. 2(b). Also here the measured and theoretical transmission agree well and a value close to the β-independent 50% level expected for the circular polarized output of an ideal effective QWP is verified.

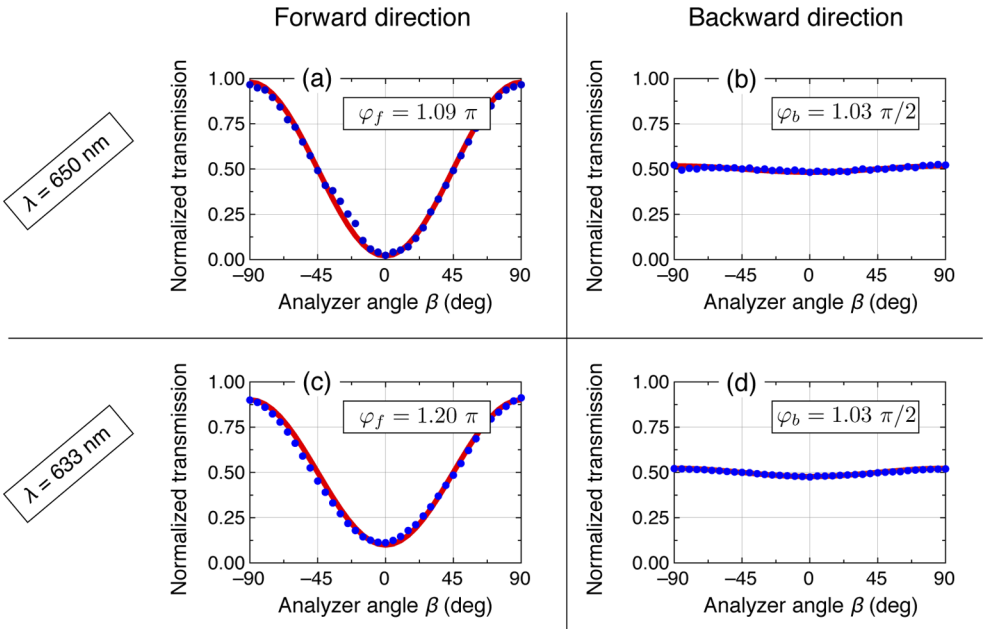

Fig. 2. Normalized transmission through the arrangement of Fig. 1(b) as a function of the analyzer orientation angle β for cases where the effective wave plate is close to a HWP in forward direction and close to a QWP in the backward one. Panels (a) and (c) are for the forward direction, (b) and (d) for the backward one. The red curves underlying the measured blue points give the theoretically expected transmission. In (a) and (b) the wavelength λ is 650 nm and the rotators angles are $\theta_1 = 26$ deg and $\theta_2 = 72$ deg, leading to phase shifts of $\varphi_f = 1.09\ \pi$ and of $\varphi_b = 1.03\ \pi/2$. In (c) and (d), $\lambda = 632.8$ nm, $\theta_1 = 30.9$ deg and $\theta_2 = 77.3$ deg, so that $\varphi_f = 1.20\ \pi$ and $\varphi_b = 1.03\ \pi/2$. The angle β is given with respect to the polarizer orientation which defines the input polarization, for $\beta = 0$ polarizer and analyzer are parallel.

If the above experiment is repeated with the 632.8 nm He-Ne laser wavelength the results are very similar. In this case the non-reciprocal rotation angle is $\theta_2 = 77.3$ deg. The corresponding experimental and theoretical normalized transmitted powers obtained upon choosing an angle $\theta_1 = 30.9$ deg for the RR are shown in Fig. 2(c) and 2(d) for the forward and backward directions, respectively. In this case the forward phase shift is $\varphi_f = 2\theta_f = 1.20 \times \pi$ and the backward phase shift is still $\varphi_b = 1.03 \times \pi/2$ close to a QWP. The comparison of Fig. 2(a) with Fig. 2(c) confirms that at 632.8 nm the structure in forward direction departs more from an effective HWP, what results in a stronger elliptical component of the output polarization and a smaller modulation of the transmission upon rotation of the analyzer. Indeed, the degree of linear polarization ξ

OSA CONTINUUM

corresponds to the fringe contrast of such a measurement [27] and decreases in forward direction from 96% to 80% going from the case of Fig. 2(a) to the one of Fig. 2(c).

Finally, an interesting and useful case is the one where the system acts in one direction as a neutral element (null retarder) that leaves the polarization unchanged. If we keep the wavelength at λ =632.8 nm this can be achieved by adjusting the RR so that $\theta_1 = \theta_2 = 77.3$ deg. This leads to $\varphi_b = 0$ and $\varphi_f = 1.72 \times \pi$, thus a null retarder in backward direction and, for our choice of wavelength and of the angle θ_2, a general retarder for the forward one. Note that in this specific case the relative phase shift in forward direction is close to the one that would be obtained by a waveplate of thickness half the one of a zero-order quarter-wave plate (λ/8-plate). The corresponding results showing the modulation of the transmitted intensity upon rotation of the analyzer are shown in Fig. 3(a) and 3(b), respectively. Clearly, as expected for such an arbitrary retarder in forward direction the output polarization is highly elliptical and the degree of linear polarization decreases here to $\xi = 49\%$. In contrast, for the null retarder in backward direction (Fig. 3(b)) the modulation is complete with a maximum transmission when polarizer and analyzer are parallel ($\beta = 0$) and a corresponding degree of linear polarization of 98%. Note that in Fig. 3(a) (as well as in Fig. 2(c)) there is a small lateral shift between the experimental data and the red curves. This is due to a small rotation of the crossed QWP for the 633 nm wavelength with respect to the x and y laboratory axes, so that the effective resulting waveplate is oriented at an angle slightly differing from the 45 deg corresponding to the theoretical red curves. The absence of this shift in backward direction (Fig. 3(b)) further confirms the action as a null retarder, for which every orientation is equivalent.

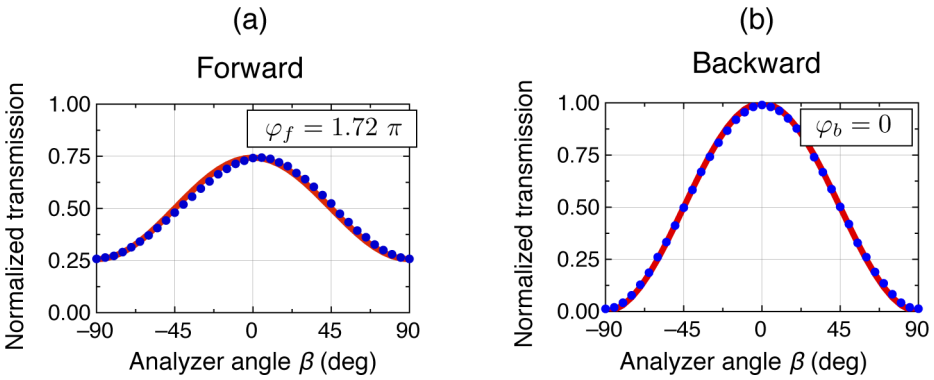

Fig. 3. Same as Fig. 2 for the case where the effective wave plate has a general retardation value (close to a λ/8-plate) in forward direction (a) and is a neutral null retarder in backward direction (b). Here $\lambda = 632.8$ nm and $\theta_1 = \theta_2 = 77.3$ deg, so that $\varphi_f = 1.72\ \pi$ and $\varphi_b = 0$.

4. Discussion and conclusions

We have presented a universal design of a non-reciprocal wave retarder based on a combination of a reciprocal and a non-reciprocal polarization rotator with two quarter-wave plates. The proof-of-concept was successfully verified experimentally for a few useful cases. The phase shifts in forward and backward directions can be adjusted by varying the reciprocal and non-reciprocal rotation angles θ_1 and θ_2. In our tests the reciprocal rotator was implemented by using a pair of half-wave plates. It is worth noting that this pair of elements may be replaced by a plate of an optically active crystal such as quartz, at the expense of a loss of tunability of the angle θ_1. The presently proposed design can find applications whenever a different manipulation of the light polarization state in two opposite directions is of interest. For instance, polarimetric analysis can take advantage of injecting the same input polarization state on both opposite ports, permitting

OSA CONTINUUM

to duplicate polarization manipulation and analysis in a single device. Novel types of optical isolators or circulators can also be envisaged. Furthermore, since for polarization encoded q-bits wave plates can take the role of various quantum gates [24], the present approach may be used also to realize different quantum optical gates in a single device, for instance a X gate in one direction and a Hadamard gate in the other. Finally, by exploiting the dispersion of the underlying reciprocal and non-reciprocal elements new types of coarse wavelength sensors based on the differential response in the two directions may be conceived.

Funding. European Commission (765075); University of Sofia (80-10-12/18.03.2021).

Acknowledgments. We dedicate this article to the memory of our colleague and friend Emiliya Dimova. We thank her for her inspiration and example.

Disclosures. The authors declare no conflicts of interest.

Data availability. Data underlying the results presented in this paper are not publicly available at this time but may be obtained from the authors upon reasonable request.

References

1. E. Hecht, *Optics* (Addison Wesley, San Francisco, 2002).
2. M. A. Azzam and N. M. Bashara, *Ellipsometry and Polarized Light* (North Holland, Amsterdam, 1977).
3. D. Goldstein and E. Collett, *Polarized Light* (Marcel Dekker, New York, 2003).
4. R. J. Potton, "Reciprocity in optics," Rep. Prog. Phys. **67**(5), 717–754 (2004).
5. D. Jalas, A. Petrov, M. Eich, W. Freude, S. Fan, Z. Yu, R. Baets, M. Popovic, A. Melloni, J. D. Joannopoulos, M. Vanwolleghem, C. R. Doerr, and H. Renner, "What is - and what is not - an optical isolator," Nat. Photonics **7**(8), 579–582 (2013).
6. M. Z. Zha and P. Günter, "Nonreciprocal optical transmission through photorefractive $KNbO_3$:Mn," Opt. Lett. **10**(4), 184–186 (1985).
7. K. A. Stankov, V. P. Tzolov, and M. G. Mirkov, "Nonreciprocal optical device based on second-harmonic generation," Appl. Opt. **31**(24), 5003–5009 (1992).
8. K. Gallo, G. Assanto, K. R. Parameswaran, and M. M. Fejer, "All-optical diode in a periodically poled lithium niobate waveguide," Appl. Phys. Lett. **79**(3), 314–316 (2001).
9. I. O. Zolotovskii and D. I. Sementsov, "Nonreciprocal effects in active nonlinear optical fibers with nonlinearity dispersion," Opt. Spectrosc. **101**(3), 446–449 (2006).
10. M. Krause, H. Renner, and E. Brinkmeyer, "Optical isolation in silicon waveguides based on nonreciprocal Raman amplification," Electron. Lett. **44**(11), 691–693 (2008).
11. Z. Yu and S. Fan, "Complete optical isolation created by indirect interband photonic transitions," Nat. Photonics **3**(2), 91–94 (2009).
12. R. Fleury, D. L. Sounas, and A. Alù, "Non-reciprocal optical mirrors based on spatio-temporal acousto-optic modulation," J. Opt. **20**(3), 034007 (2018).
13. J. Wang, Y. Shi, and S. Fan, "Non-reciprocal polarization rotation using dynamic refractive index modulation," Opt. Express **28**(8), 11974–11982 (2020).
14. J.-M. Liu, *Photonic Devices* (Cambridge University, Cambridge, 2005).
15. Y. Okamura, T. Negami, and S. Yamamoto, "Integrated optical isolator and circulator using nonreciprocal phase shifters: a proposal," Appl. Opt. **23**(11), 1886–1889 (1984).
16. O. Zhuromskyy, H. Dotsch, M. Lohmeyer, L. Wilkens, and P. Hertel, "Magnetooptical waveguides with polarization-independent nonreciprocal phase shift," J. Lightwave Technol. **19**(2), 214–221 (2001).
17. H. Yokoi, T. Mizumoto, N. Shinjo, N. Futakuchi, and Y. Nakano, "Demonstration of an optical isolator with a semiconductor guiding layer that was obtained by use of a nonreciprocal phase shift," Appl. Opt. **39**(33), 6158–6164 (2000).
18. Y. Shoji, I. Hsieh, R. Osgood Jr., and T. Mizumoto, "Polarization-independent magneto-optical waveguide isolator using TM-mode nonreciprocal phase shift," J. Lightwave Technol. **25**(10), 3108–3113 (2007).
19. E. Ishida, K. Miura, Y. Shoji, H. Yokoi, T. Mizumoto, N. Nishiyama, and S. Arai, "Amorphous-si waveguide on a garnet magneto-optical isolator with a TE mode nonreciprocal phase shift," Opt. Express **25**(1), 452–462 (2017).
20. P. Pintus, D. Huang, P. A. Morton, Y. Shoji, T. Mizumoto, and J. E. Bowers, "Broadband TE optical isolators and circulators in silicon photonics through Ce:YIG bonding," J. Lightwave Technol. **37**(5), 1463–1473 (2019).
21. E. Dimova, A. A. Rangelov, and E. Kyoseva, "Tunable bandwidth optical rotator," Photonics Res. **3**(4), 177 (2015).
22. A. A. Rangelov and E. Kyoseva, "Broadband composite polarization rotator," Opt. Commun. **338**, 574–577 (2015).
23. A. Messaadi, M. M. Sanchez-Lopez, A. Vargas, P. Garcia-Martinez, and I. Moreno, "Achromatic linear retarder with tunable retardance," Opt. Lett. **43**(14), 3277–3280 (2018).
24. M. A. Nielsen and I. L. Chuang, *Quantum Computation and Quantum Information* (Cambridge University, Cambridge, 2000).
25. J. C. Suits, B. E. Argyle, and M. J. Freiser, "Magneto-optical properties of materials containing divalent Europium," J. Appl. Phys. **37**(3), 1391–1397 (1966).

OSA CONTINUUM

26. V. Vasyliev, E. G. Villora, M. Nakamura, Y. Sugahara, and K. Shimamura, "UV-visible Faraday rotators based on rare-earth fluoride single crystals: $LiREF_4$ (RE = Tb, Dy, Ho, Er and Yb), PrF_3 and CeF_3," Opt. Express **20**(13), 14460–14470 (2012).
27. M. Al-Mahmoud, V. Coda, A. A. Rangelov, and G. Montemezzani, "Broadband polarization rotator with tunable rotation angle composed of three wave plates," Phys. Rev. Appl. **13**(1), 014048 (2020).